World Academy of Science, Engineering and Technology
International Journal of Geological and Environmental Engineering
Vol:11, No:4, 2017

Numerical Modelling of Shear Zone and Its Implications on Slope Instability at Letšeng Diamond Open Pit Mine, Lesotho

M. Ntšolo, D. Kalumba, N. Lefu, G. Letlatsa

***Abstract*—**Rock mass damage due to shear tectonic activity has been investigated largely in geoscience where fluid transport is of major interest. However, little has been studied on the effect of shear zones on rock mass behavior and its impact on stability of rock slopes. At Letšeng Diamonds open pit mine in Lesotho, the shear zone composed of sheared kimberlite material, calcite and altered basalt is forming part of the haul ramp into the main pit cut 3. The alarming rate at which the shear zone is deteriorating has triggered concerns about both local and global stability of pit the walls. This study presents the numerical modelling of the open pit slope affected by shear zone at Letšeng Diamond Mine (LDM). Analysis of the slope involved development of the slope model by using a two-dimensional finite element code RS2. Interfaces between shear zone and host rock were represented by special joint elements incorporated in the finite element code. The analysis of structural geological mapping data provided a good platform to understand the joint network. Major joints including shear zone were incorporated into the model for simulation. This approach proved successful by demonstrating that continuum modelling can be used to evaluate evolution of stresses, strain, plastic yielding and failure mechanisms that are consistent with field observations. Structural control due to geological shear zone structure proved to be important in its location, size and orientation. Furthermore, the model analyzed slope deformation and sliding possibility along shear zone interfaces. This type of approach can predict shear zone deformation and failure mechanism, hence mitigation strategies can be deployed for safety of human lives and property within mine pits.

***Keywords*—**Numerical modeling, open pit mine, shear zone, slope stability.

I. Introduction

THE surrounding geology around rock engineering projects has been accepted as the most significant factor in the design of both surface and underground excavations. The surrounding geology could include tectonic structures like folds, faults, and shear zones which have been associated with slope failures before [1]. Therefore, it is crucial to evaluate the influence of these structures when encountered in rock engineering projects.

One of these tectonic structures which has been studied more in geosciences where fluid transport is of major interest is shear zones. In contrast, the role played by shear zones in the open pit mine slope instabilities is still desired in the field of rock engineering and structural geology. Therefore, it is critical to fully understand the behavior of shear zones rock mass and find the best approach to model their impact in excavated slopes in order to avoid causalities and reduction in shareholders' returns.

At Letšeng Diamond open pit mine, the shear zone cuts across two pits (Main and satellite pits) as illustrated in Fig. 1. The failures around and on this zone are a major concern for mine management as it puts both mine workers and machinery at risk when working on its vicinity. The purpose of this research is to analyze the shear zone and its failure mechanism in order to predict pit failures associated with shear zone when pits are getting deeper.

II. Letšeng Diamonds Location

LDM is located approximately 217 km north east of the capital town (Maseru) in Lesotho. Lesotho is a country bounded by South Africa as shown in Fig. 2. Diamond mining is practiced at approximately 3100 m altitude, and according to [2], LDM is regarded as the highest diamond open pit mine in the world. At this mining area, the temperatures can drop as low as -20 °C in winter which is a big challenge for mining activities in winter season.

III. Geological Setting on Mining Area

LDM lies on the high elevated Drakensburg range mountains which belongs to Drakensberg Group (187 Ma – 155 Ma) [3] that consists of basaltic lavas referred as the Lesotho Formation of Karoo Supergroup. The Karoo sequence has been extensively intruded by diamondiferous kimberlite pipes, dykes, and dolorite sills on the northern part of Lesotho known as Northern Lesotho Kimberlite Field (NLKF) [4]. In this area, kimberlite pipes rich of diamonds intruded as twin pipes (main and satellite) at four locations: Liqhobong, Kao, Letšeng, and Mothae.

The stratigraphy of NLKF consists of shale and sandstones that belong to Molteno Formation. This layer is then overlain by sandstones of the Clarens Formation. Clarens Formation is then overlaid by basaltic lavas of Lesotho formation which forms the country rock while dolerite and kimberlite dykes' extrusion cuts through them [2].

At Letšeng diamonds, two kimberlite pipes intruded in close proximity to one another as main and satellite kimberlite pipes (Fig. 3). Satellite pipe is smaller in size compared to main pipe. Satellite pipe consists of basalt raft and two kimberlite facies: North Volcanoclastic Kimberlite (NVK) and South Volcanoclastic Kimberlite (SVK). On the other hand,

Motheo Ntsolo is with the University of Cape Town, South Africa (e-mail: ntsmot003@myuct.ac.za).

the main pipe is subdivided into three kimberlite facies: K main, K6, and K4, but it also has basalt raft similar to satellite pipe. The Letšeng kimberlite pipes are vertical cone shape [5], while a sharp contact between kimberlite and basalt was observed in satellite pit. The sharp contact in this context means a rapid change in sediment types. The kimberlites comprise of volatile, potassic, and ultrabasic rock with an inequigranular texture that results from phenocrysts and xenoliths being set in a fine-grained matrix [5].

Fig. 1 Shear Zone Across Satellite and Main Pits at Letšeng Diamonds Mine in Lesotho

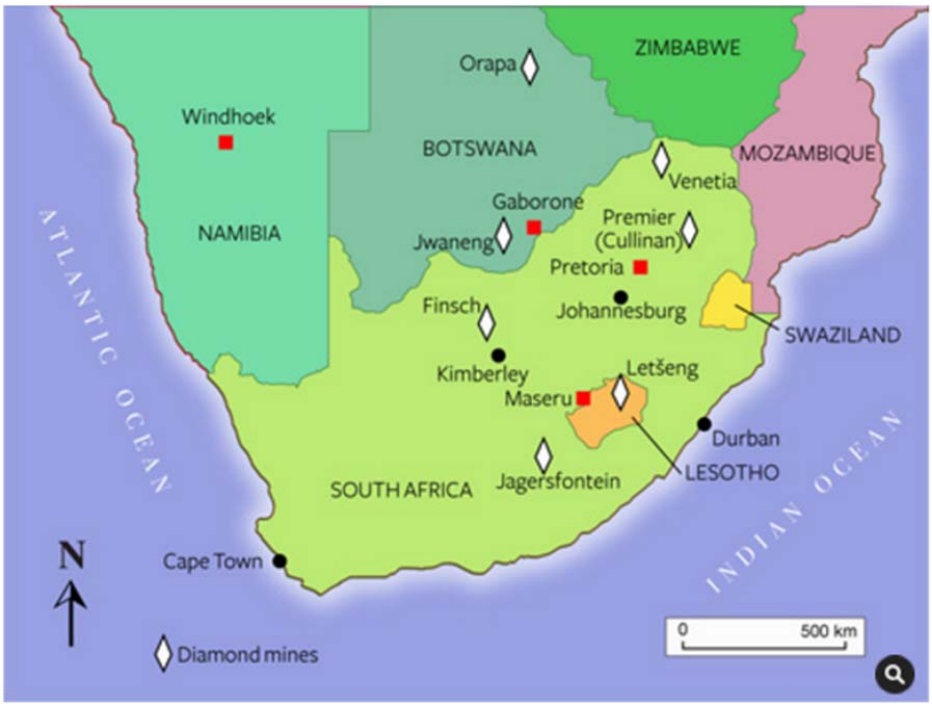

Fig. 2 LDM Locality Map [6]

IV. Mining at LDM

Diamond mining is conducted on two diamondiferous kimberlite pipes ore bodies (Main and Satellite) very close to each other which extruded in basalt country rock. At LDM, the pipes are mined simultaneously as Main and Satellite pits by pre-split blasting, loading, and hauling trucks. Both pits are currently (2016) at an average depth of 180 m from the surface. Even though ore bodies are regarded as low grade (1-3.5 carats/hundred ton), the mine is famous of producing large high value diamonds. One example of large recovered

diamond is “Letšeng Star” which was recovered in 2011, and it was 550 carats diamond with average value of US$16M [6].

In the process of exploiting these two kimberlite pipes, blasting excavation is done through basalt country rock which is massive and strong in nature. However, discontinuities subjected to basalt rock limit its brittle deformation. The excavations cut through these joints, but more importantly through a sensitive zone composed of intensively sheared kimberlite, calcite, and basalt matrix. This zone is called shear zone. It is very unstable and is a major concern for geotechnical team within the mine.

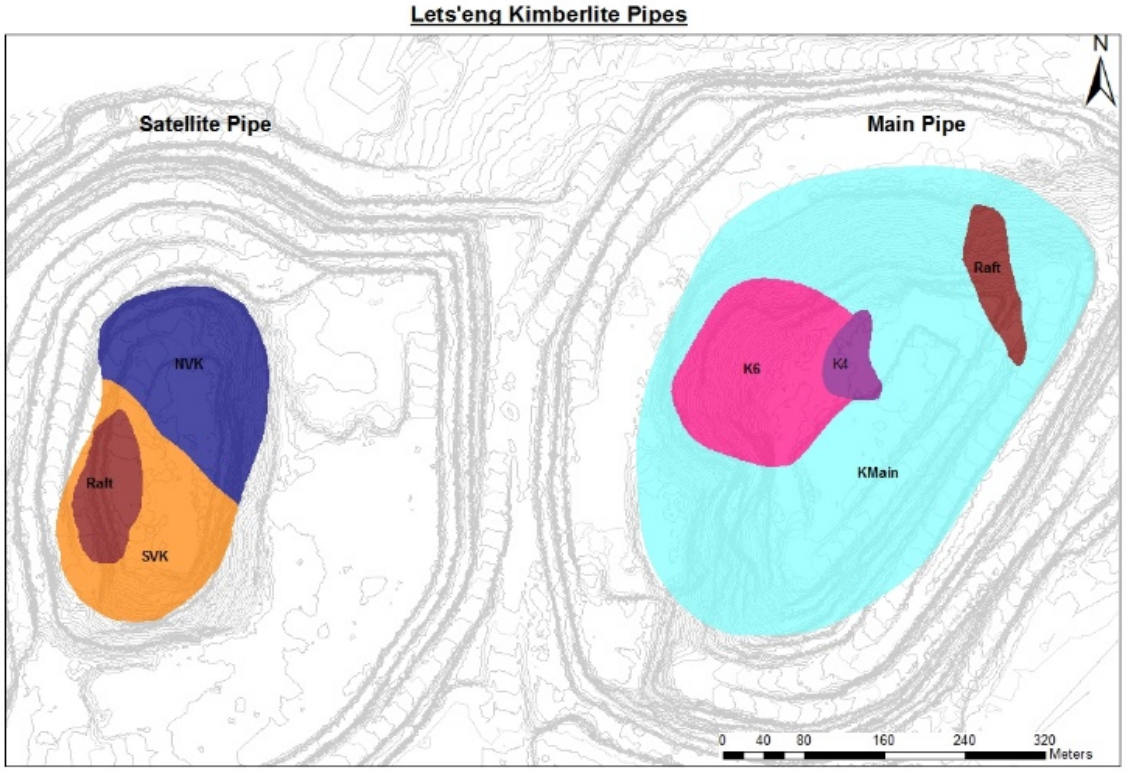

Fig. 3 Main and Satellite Kimberlite Pipes at LDM

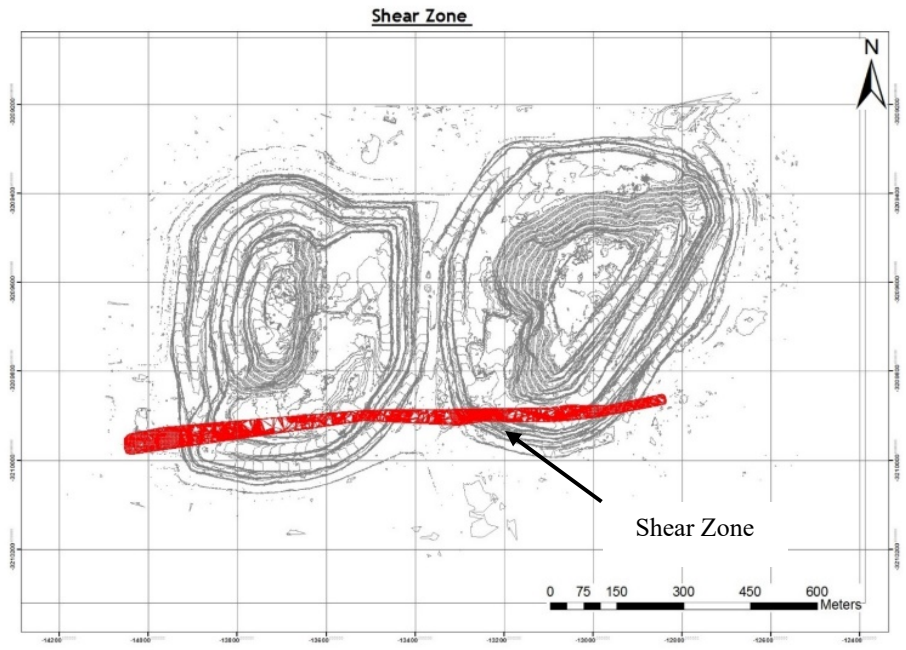

Fig. 4 Location of LDMSZ on Main and satellite pits

V. Materials and Methods

A. Shear Zone Description

LDM shear zone (LDMSZ) is a complex geological structure that cuts towards southern edges of both satellite and main pits (Fig. 4). The thickness of LDMSZ was measured from exposed surfaces in both pits and it varies considerably in the range of 15 to 35 m, it strikes NE – SW direction and the inside joints deep steeply at an average of 75°/220° (dip angle/dip direction).

The rock mass in the shear zone exhibits crushed and brecciated structure which, according to [7], is a sign of displacement not confined to one fracture, instead, distributed throughout the shear zone. Fig. 5 shows shear zone in Main Pit Cut 3 West (MPC3W) between host rock together with a dyke at the right side of shear zone. The joints strike in the same direction with shear zone but converge to rock mass matric towards middle of slope. The thickness is larger at the bottom and decreases upwards.

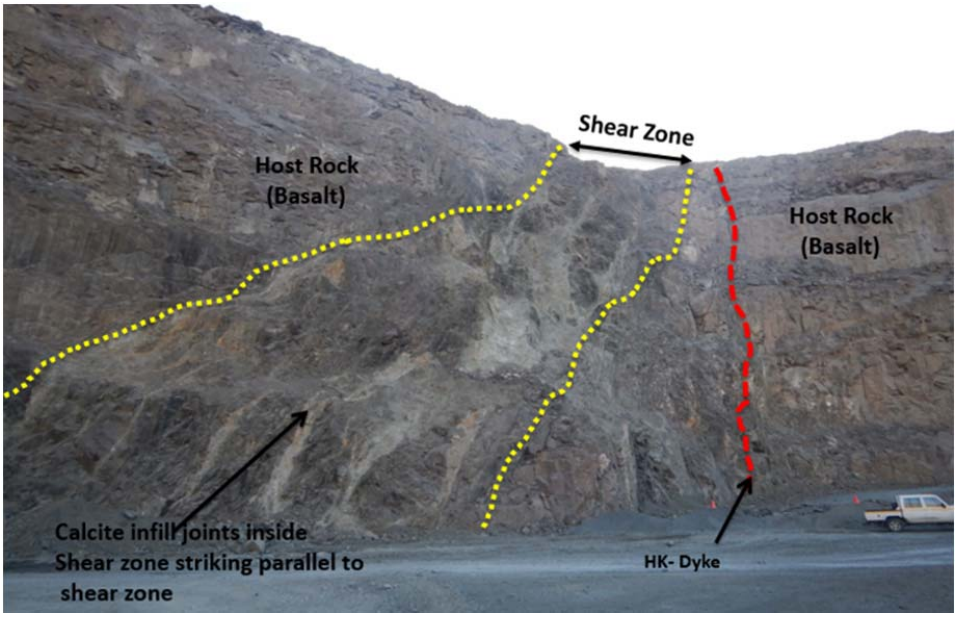

Fig. 5 MPC3W Shear Zone Showing Deformation Complexity

The deformation history of this shear zone is highly complex and this is marked by variable shear bands and dykes within its vicinity as shown in Fig. 5. The dyke in Fig. 5 runs close to shear zone and can be observed on the on the other side of the slope in satellite pit. Detailed observations conducted during mapping, and core logging shows displacement to have occurred along closely spaced network of fractures. The high permeability of fractured material highlights promotion of hydrothermal inflow and according to [8], shearing is often accompanied by hydrothermal activities. In addition, the shear zone shows higher fracture density than the host rock (basalt). Joints inside the shear zone are closely spaced (5 to 20cm); the joints-infilled material is composed of sheared and structureless fine grained rock mass. The highest fracture densities are demonstrated by fine grained sections of the shear zone. This was observed in MPC3E where highly deteriorating shear zone material is forming base of the haul ramp. The thickness of the fracture infill generally increases towards areas of high fracture densities in MPC3E shear zone, which is from the edges towards middle of shear zone. This observation further proves observation made by [8] that shear intensity is usually from the centre of shear zone reducing away towards the edges.

The geological development of LDMSZ is not clearly defined. However, shear zones are tectonic structures which are related to kimberlite locations. Vearncombe and Vearncombe [9] analyzed vast amount of data collected from different kimberlite locations in southern Africa and proved that different strips of kimberlites are parallel to prominent shear zones and faults in the Archaean-Kaapvaal craton. These shear zones close to kimberlite pipes are believed to have been formed during relatively slow emplacement of diamonds which fails to penetrate the whole Earth's crust, thus creating heterogeneous and weak zone called shear zone [9]. The location (parallel to kimberlite pipes) and presence of sheared kimberlite inside LDMSZ somehow proves the hypothesis made by [9].

B. Field Investigation

The study of shear zone at Letšeng diamond commenced with geological and geotechnical mapping. It was the objective of this study to conduct both face and scanline mapping on all exposed shear zone faces; however, due to unstable nature of the shear zone and its sudden failure, only selected safe faces were mapped due to safety reasons. The mapping included both face and scanline mapping. Scanline mapping is a suitable method for determining discontinuity orientation and any other geometrical properties on the exposed surfaces [10]. For these reasons, scanline mapping was conducted on the exposed and accessible shear zone on

MC3E in accordance to Laubscher's Rock Mass Rating (RMRL90) System [11]. It should be emphasized that Geological Strength Index (GSI) and Rock Quality Designation (RQD) estimation were also included in scanline mapping.

At the beginning of this study, a total of 34 drill holes were already drilled between 2011 and 2014 (LDM records) on both pits, logged and analyzed by geotechnical team on site. Since the main purpose of this study was on the shear zone, six out of 34 drill cores that cut through shear zone were recovered from store and re-logged with more interest on the shear zone. Analysis of drill cores provided data on orientation of structures, fractures, and infilling material inside and around shear zone. The borehole data collected included the identification of the geotechnical interval, the rock type unit, the values of intact rock strength (IRS), hardness rating (UCS), fracture frequency (FF) and joint condition rating (JCr) which includes micro and macro conditions. Finally, the parameters recorded were Laubscher's Rock Mass Rating (RMR_{L90}) used for rock mass classification.

C. Rock Mass Classification

According to Bieniawski [12], one of the objectives of rock mass classification is to derive quantitative data for engineering design. To derive these data, geotechnical parameters obtained from mapping and core logging of shear zone and surrounding structures were analyzed by three rock mass classification systems: RQD, Laubscher Rock Mass Rating (RMR_{L90}) and Hoek and Brown's GSI.

The RQD values were estimated from face mapping and calculated from core logging data by using method suggested by [14] and presented by (1).

$$\text{RQD} = \frac{\sum \text{Length of core pieces} > 100\text{mm length}}{\text{Total length of core run}} \quad (1)$$

Hudson and Priest [13] presented another method of estimating RQD from face mapping as in (2).

$$\text{RQD} = 100\, e^{-0.1\lambda}(1 + 0.1\lambda) \quad (2)$$

where λ = the total joint frequency.

Equation (2) was also used to estimate RQD from FF. Since the shear zone has more than a 1-m thickness, it was analyzed separately as suggested by [11]. Table I shows results of RQD for shear zone from 6-borehole logging and the average of 32.5 is regarded as poor rock [12].

TABLE I
SHEAR ZONE RQD

	Min	Max	Mean	Std dev.	Class
RMR	0	60	32.5	27	Poor rock

To characterize the lithological units of shear zone, RMR_{L90} system was adopted as in (3).

$$RMR_{L90} = \text{IRSr} + \text{FFr} + \text{JC} \quad (3)$$

where: IRSr is the IRS rating, derived from synchronising laboratory tests, field test and estimated from core logging. FFr is the FF rating, and JCr is the joint condition and water rating. Joint condition includes joint roughness (both macro and micro scale), joint infill conditions, and joint wall alteration condition.

Table II shows results of RMR for shear zone from 6-borehole logging, and the average of 37.3 is regarded as poor rock [11].

TABLE II
SHEAR ZONE RMR

	Min	Max	Mean	Std dev.	Class
RMR	22.9	60.3	37.3	11.9	Poor rock

In order to consider the effects of weathering, joint orientation, blasting and stress, RMR_{L90} is adjusted to Mine Rock Mass Rating (MRMR) as proposed by [11] in (4). The adjustments and justification used specifically for this study are presented in Table III. Equation (4) shows how MRMR was determined by adjusting RMR. An example of these adjustment factors could be an induced mining stress, where induced stresses can result from redistribution of regional stress caused by pit geometry and orientation of excavation. At LDM the geometry of the pit is concave; therefore, effect of any stress relaxation will be balanced. Hence, no adjustment factor for mining induced stress in this analysis.

$$MRMR = \text{RMR} \times \text{Aw} \times \text{Ajo} \times \text{As} \times \text{Ab} \quad (4)$$

TABLE III
SHEAR ZONE RMR

Adjust.	Abbrev.	Range	Justification
Weathering	Aw	75%	Weathered rock
Joint orientation	Ajo	85%	Unfavorable jointing
Stresses	As	100%	No stress effect
Blasting	Ab	90%	High fracture density

In order to compare shear zone rock mass with the country rock, Table IV summaries characteristics of basalt rock with shear zone rock mass. It can be noted from Table IV that shear zone rock mass is very weak as compared to basalt rock by exhibiting low RQD and RMR values.

NB: Basalt rock parameters were obtained from mine records.

TABLE IV
SHEAR ZONE RMR

Rock Type		RQD (%)	IRS (MPa)	IRS (rating)	FF	Jc	RMR
Basalt	mean	97	174	18	36	28	82
	min	0	2	1.5	4	1.5	23
	max	100	185	20	40	40	100
	stdev	10	23	3	6	9	14
Shear zone	mean	32.5	95.3	10.6	13.9	12.8	37.3
	min	0	18	3	2.3	5.9	22.9
	max	60	185	20	21	23.3	60.3
	Stdev.	27	67.8	6.8	6.2	5.9	11.9

GSI values were estimated by using Hoek-Brown rock mass

classification chart developed for heterogeneous rock mass by [15]. This was based on the fact that the shear zone was tectonically deformed rock mass. Moreover, geological observations like joint density, weathering, and tectonical deformation are captured in this type of GSI classification method. In addition to estimating GIS by visual inspection, GSI values were estimated during core logging based on the conversion proposed by [16] as presented in (5).

$$GSI = 1.5\,JC + \text{RQD}/2 \tag{5}$$

Given the average joint condition (Jc) of 12.8 and RQD of 32.5, (5) above gave GSI of 35.5 which falls in the range of GSI estimated from field observations.

D. Estimation of Rock Mass Properties

In rock masses of defined discontinuities, the behavior of rock mass is anisotropic, and failure is controlled by discontinuities which act as release surfaces [15]. However, if rock mass is heavily fractured and crushed, the continuity of discontinuities is disrupted, and rock mass behaves as isotropic mass [15]. To consider effect of fractured rock mass, GSI which was developed originally by [17] and later modified by [15] for heterogeneous rock masses, provides a method of relating geological observation in the field to rock mass quality as presented in previous section. Furthermore, GSI can be extended to estimate in-situ rock mass strength and characteristics in Hoek-Brown failure criterion. This application demonstrates the importance of GIS from classification systems to input parameter in geotechnical behavior of rock masses.

Rock mass strength parameters were analyzed by the non-linear Hoek-Brown criterion that relates the strength envelope to the rock mass classification through the GSI called Generalized Hoek-Brown failure criterion [15] in (6).

$$\sigma_1' = \sigma_3' + \sigma_{ci}\left(m_b \frac{\sigma_3'}{\sigma_{ci}} + s\right)^a \tag{6}$$

where σ_1' and σ_3' are the axial and confining effective stresses a failure, σ_{ci} is the unconfined compressive strength of intact rock (UCS), m_b, s, and a are related to the rock mass rating through GSI.

The relationship of m_b, s and a are expressed in [18] as (7), (8) and (9), respectively.

$$m_b = m_i \exp\left(\frac{GSI - 100}{28 - 14\,D}\right) \tag{7}$$

$$s = \exp\left(\frac{GSI - 100}{9 - 3D}\right) \tag{8}$$

$$a = \frac{1}{2} + \frac{1}{6}\left(e^{-GSI/15} - e^{-20/3}\right) \tag{9}$$

where: m_i is a material constant and D is Disturbance Factor.

In addition to GSI values discussed above, it is necessary to consider the selection of "intact" rock mass properties σ_{ci} and m_i for heterogeneous rock masses. The intact compressive strength UCS is usually determined from the laboratory tests; however, in weak heterogeneous rock masses like shear zones in Fig. 6, it is difficult to recover samples for testing. For example, the thin basalts and kimberlite beds in Fig. 6 show heterogeneity, the complexity of the formation, and the difficulty in estimating intact rock properties. Therefore, UCS values were estimated from published correlation tables such as those of International Society for Rock Mechanics.

Fig. 6 Tectonically Heavily Sheared Alteration of Green Kimberlite and Grey Basalt at MC3W

Disturbance factor (D) ranges from D = 0 for undisturbed rock masses to D =1 for completely disturbed rock mass due to blast damage and stress relaxation. Disturbance factor of 0.8 was considered due to low intact strength of shear zone material.

Shear zones more than 1 m must be treated separately [19]. Therefore, the contact between shear zone and host rock (basalt) creates an interface which needs to be incorporated in the analysis. A regularized Coulomb friction law simulates the mechanical response of interfaces [20]. The Mohr-Coulomb elastic perfectly-plastic slip criterion was adopted in this study for joint behavior. This means that the joints in the interface were allowed to slip. The contact interface is represented by shear modulus and joint stiffness values which were estimated by relations proposed by [21]. The joint and interface geomechanical parameters used in this study are presented in Table V.

TABLE V
GEOMECHANICAL PARAMETERS USED FOR JOINTS

Joint	Shear stiffness, KS (MPa/m)	Normal stiffness, KN (MPa/m)	Frictional angle, ∅ (°)	Cohesion c (MPa)	Tensile strength (MPa)
J1	2398	6477	43	0	0
J2	776	1122	32	0	0
J3	1679	4534	34	0	0

J1: shear zone-to-Basalt interface, J2: shear zone inside joints, and J3: Kimberlite-to-Basalt interface

Finally, the shear strength parameters for shear zone material were obtained by using relationships between Hoek-Brown and Mohr – Coulomb criterion through use of Rockdata v5.0 [22]. The results used as input data in stability analysis are summarized in Table VI. Basalt and kimberlite properties were obtained from mine records.

TABLE VI
BASALT, SHEAR ZONE AND KIMBERLITE STRENGTH PARAMETERS

	GSI	D	mi	mb	s	a	σ_{ci} (MPa)	E_m (MPa)	C (MPa)	Phi (°)
BS	**75**	0.7	14	3.5	0.03	0.521	135	46500	2.84	59
SZ	**32.5**	**0.8**	**11**	**0.204**	**0.00004**	**0.518**	**15**	**7500**	**0.28**	**15.9**
KB	**50**	0.8	6.9	0.351	0.0005	0.505	53.9	16170	0.35	38.1

BS-Basalt, SZ-Shear Zone and KB-Kimberlite

VI. NUMERICAL MODELLING

A. RS2 FEM-SSR Model

Numerical analysis of open pit mine slope in the highly fractured, brecciated shear zone rock masses was accomplished by using a two-dimensional hybrid element model called RS2 Finite Element Program [22] assuming plain strain conditions. This software utilizes Shear Strength Reduction (SSR) technique in stimulating factor of safety as critical reduction factor. The critical reduction factor is equivalent to slope factor of safety. In SSR, the strength parameters, cohesion (c) and frictional angle (∅), are reduced by strength reduction factors until the model becomes unstable, i.e. when analysis results are not converging. Then, the reduction factor that causes analysis not to converge is called critical reduction factor and it becomes slope factor of safety. In this simulation, elasto-plastic analysis is used to compute deformations and stresses. Model properties used in this analysis were obtained from Table VI.

B. Setting up Numerical Model

In contrast with traditional limit equilibrium methods, numerical calculations are more sensitive to boundary range [23]. To minimize the impact of boundary effects on modelling outputs, the size of the model was extended 2.5 times larger depth of both pits (2.5 H1) on both ends, model depth is 2H1 as illustrated in Fig. 7. In this way, the shear zone model is extended far enough from the excavation to eliminate external boundary effect. Originally before mining, the rock mass was in equilibrium state by gravity, mining activity released lateral constrain, thus creating open slopes. Therefore, the upper part of the model will act as free surfaces together with slope faces. The bottom of the model is fixed, while "rollers" are placed on the sides to allow vertical displacements and to restrain lateral displacement.

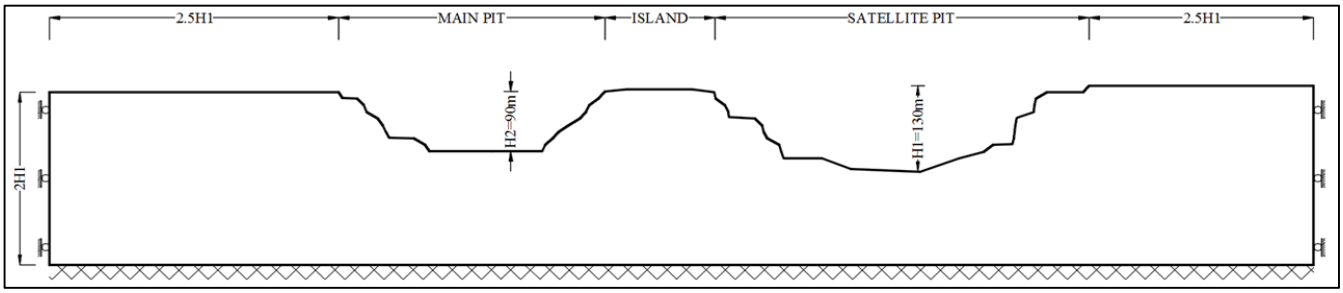

Fig. 7 Shear zone model configuration

C. Model Simulation

In the first stage, the model was calibrated by displacement measurement on site at slope in Satellite pit cut 5 east (SPC5E) as illustrated in Fig. 8. This was done by adjusting strength parameters (c and ∅) such that the model produces deformation similar to filed measured displacements. Calibrated c and ∅ were then used for further analysis.

Window mapping conducted on exposed and accessible face in MC3W indicated closely spaced joints inside shear zone dipping approximately 75° away from the slope. Kinematic analysis based on window mapping results predicted toppling failure on the same area. Even though the shear zone forming base of haul ramp in main pit was not mapped, similar joints orientation to mapped face could be observed. Therefore, shear zone was assumed to dip 75° away from slope face together with joints inside as shown Fig. 9. This section was selected for finite element analysis since signs of instabilities have been observed on site in this location. This section is located at "access ramp" indicated in Fig. 8.

The intact rock in this model for host rock is considered as linear-elastic material that follows Hoek-Brown failure criterion. In contrast, Mohr-Coulomb elasto-plastic material model was used for shear zone in order to allow for plastic deformation and failure. The joints and interfaces also follow Mohr-Coulomb failure criterion in order to evaluate the possibility of slipping failure along the joints.

To simulate the excavated slope on the shear zone, finite element model was generated by configuration in Fig. 9, and six nodded triangulated elements were used in finite element mesh to discretize the whole rock mass.

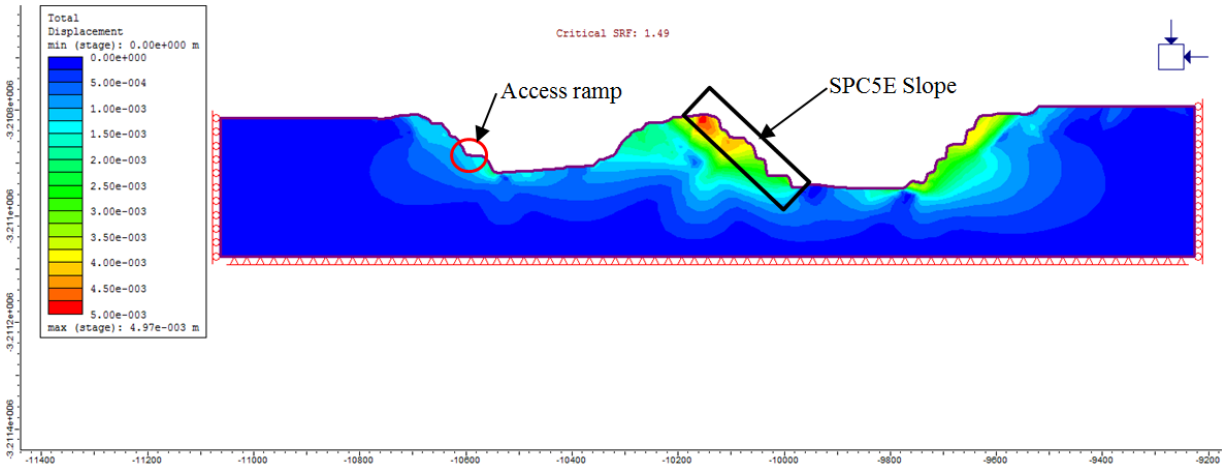

Fig. 8 Calibrated model showing deformation similar to measured displacement on the field

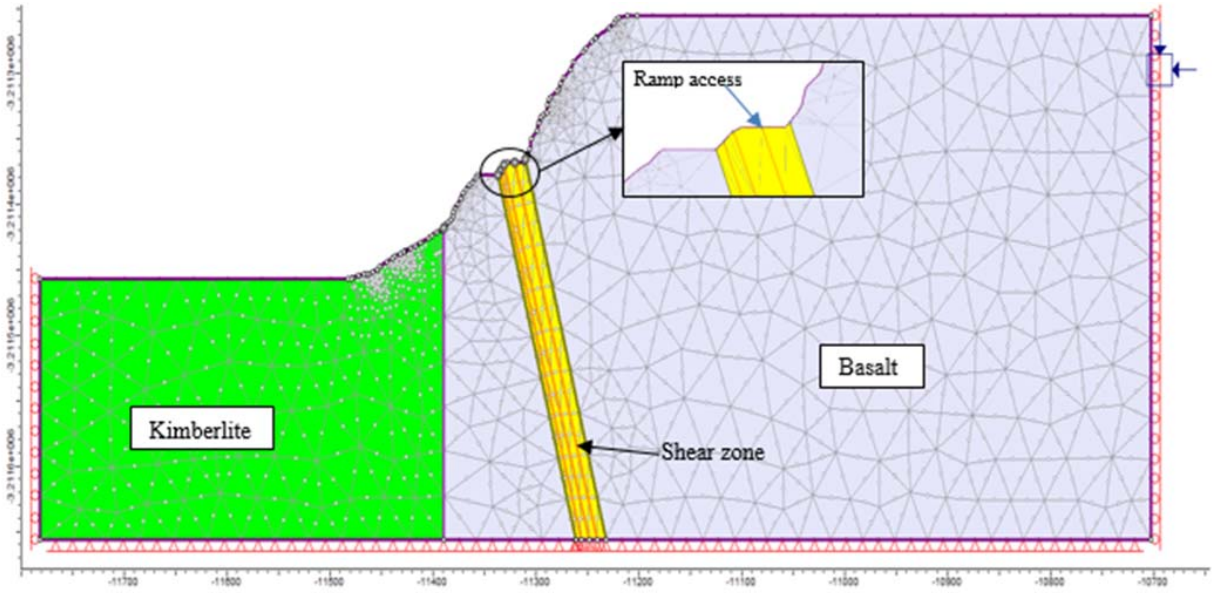

Fig. 9 Section through access ramp in MPC3E

VII. Results and Discussion

A. Critical Displacement Points

The total displacement contours generated from the model are illustrated in Fig. 10. Max total displacement of 44 mm are experienced on kimberlite at the toe of the slope (Fig. 10). Field displacement at access ramp together with calibrated displacement was 5 mm as it can be seen in Fig. 8. However, out of plane displacement shown in Fig. 10 predicts maximum displacement of 32 mm at the same location. Clearly, shear zone is more unstable on the side of larger displacements.

B. Plastic Zones or Yielding Points Distribution

The plastic zone is close to the surface on the shear zone as shown in Fig. 11. This zone indicates failed elements in finite element analysis. The plastic zone distribution in shear zone shows extensive development of stress in this zone which is concentrated towards the surface of shear zone. The largest plastic zone distance from the surface along the shear zone is approximately 56 m where both rock mass and joints have yielded. From 56 m to 120 m along inclined shear zone, only joints inside the shear zone have yielded indicating slip failure along the joints. The bottom interface joint between shear zone and basalt did not show any yielding, while upper joint showed yielding at one point towards the surface.

C. Failure Mode Mechanism

Maximum shear strain results are shown in Fig. 12 indicating mode and location of failure. From Fig. 12, kimberlite is highly strained at the toe of the slope and at interface with basalt rock mass. Shear zone shows high stress almost all the way to bottom of the model. Competent basalt remains stable and shows no signs of instability. The global factor of safety is 2.33 which is above equilibrium, hence slope can be considered safe globally [18].

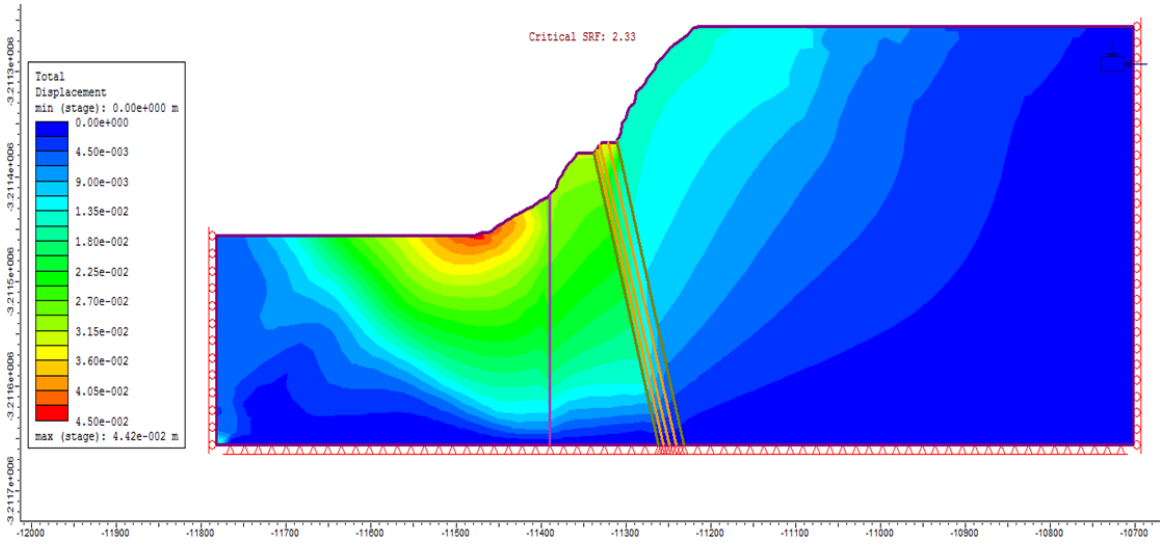

Fig. 10 Total displacement

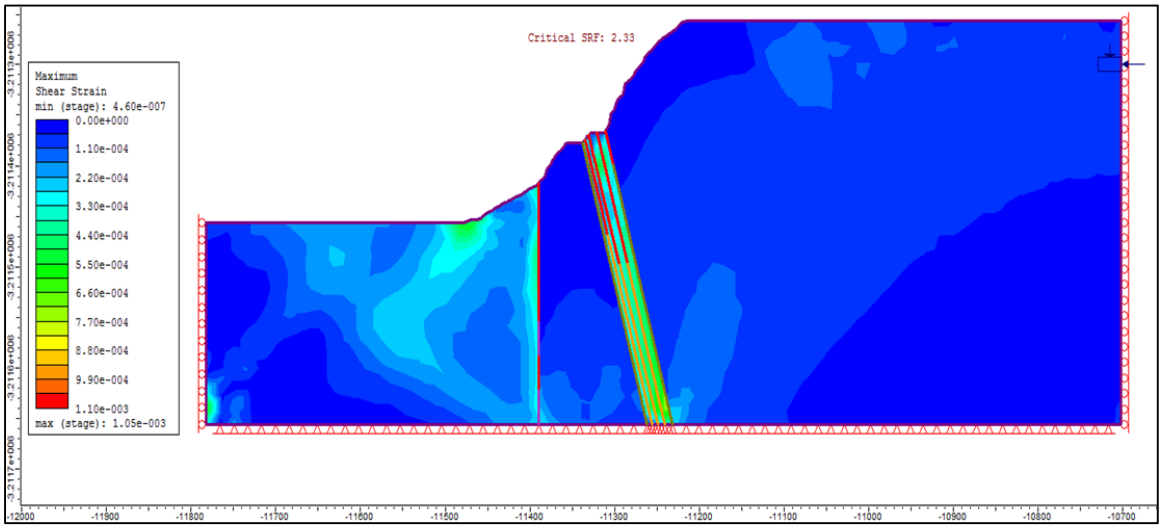

Fig. 11 Plastic zones and yielding of joints

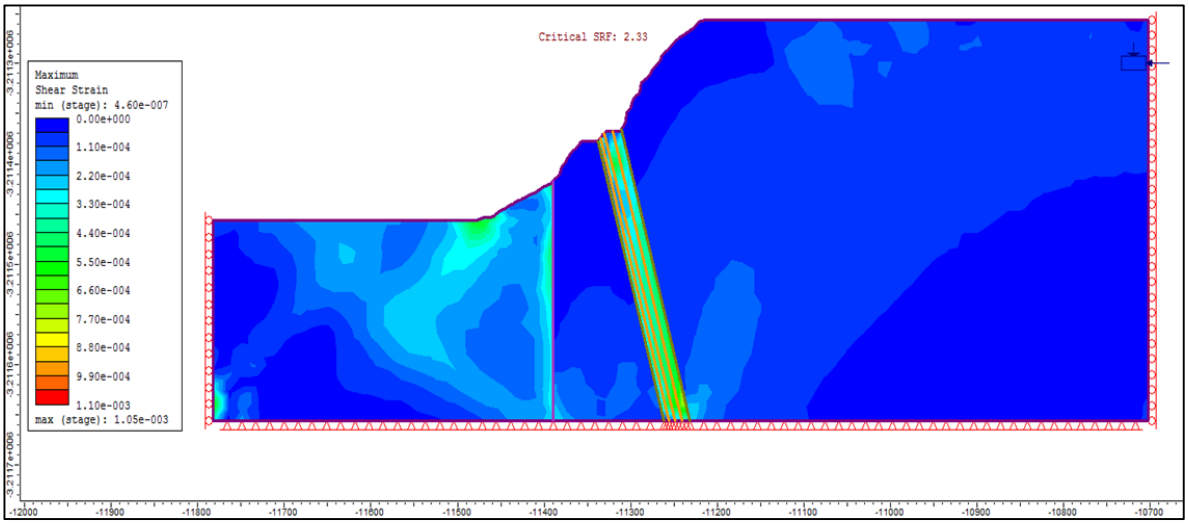

Fig. 12 Factor of safety and failure mechanism

VIII. Conclusion

Shear zone is a complex geological structure, knowledge of shear zone strength and deformability characteristic is also important to usefully incorporate shear zone in analytical and numerical analysis. The strength of shear zone was considered poor by RQD and RMR classicization systems. The whole upper part of shear zone close to access ramp was in plastic state, while basalt on either side is still intact. Therefore, any shear zone failure will be localized and will not affect the surrounding of competent basalt. This type of failure was observed in satellite pit where shear zone has failed up to its extend leaving steeply dipping competent basalt plane. The joints inside the shear zone did not play major role in controlling the failure as they were yielded together with infill material between them. This was observed where the shear zone is not confined by country rock at ramp access. It can therefore be concluded that, when the shear zone is exposed to environment unsupported or unconfined at one side, it will deteriorate without the influence of joints inside it up to the interface with the competent rock mass face or supporting structure.

The results from finite element analysis were consistent with field observations, hence demonstrating abilities of continuum modeling in analyzing discontinuous rock mass through special joint element code. With adequate data for input parameters and proper calibration of models, numerical modelling can be a useful tool for predicting failure modes of rock masses, hence mitigation strategies can be provided prior to failure.

Due to unstable nature of shear zone, it is recommended to make proper monitoring system deployed on site not only for signal during failure but also for adequate calibration of numerical models.

The future work for this study is to investigate appropriate support system on the unstable shear zone. The research should consider the applicability of proposed solution on site as at some locations, basalt rock mass on the vicinity of shear zone is highly fractured.

References

[1] T. C. Badger, *Fracturing within anticlines and its kinematic control on slope stability*. Environmental & Engineering Geoscience. 2002;8(1):19-33.

[2] D. C. Bowen, R. D. Ferraris, C.E. Palmer, J. D. Ward. *On the unusual characteristics of the diamonds from Letšeng-la-Terae kimberlites, Lesotho*. Lithos. 2009; 112:767-74.

[3] M. Lephatsoe, E. Hingston, M. Ferentinou, N. Lefu. *Kinematic Analyses of the Western Pitwall of the Main Pit in the Letseng Diamond Mine, Lesotho*. ISRM Regional Symposium-EUROCK 2014; International Society for Rock Mechanics; 2014.

[4] F. Reichhardt, M. Lynn. *Lemphane kimberlite technical report*. Ni 43-101 Independent Technical Report on the Lephane Kimberlite Project, Lesotho. 2010;19-21; unpublished.

[5] A. Madowe. *The mine planning process for an open-pit diamond mining operation-a case study on Letseng diamond mine in Lesotho*. Journal of the Southern African Institute of Mining and Metallurgy. 2013;113(7):547-54.

[6] R. Shor, R. Weldon, A. Janse, C. M. Breeding, S. B. Shirey. *Letšeng's Unique Diamond Proposition*. Gems & Gemology. 2015;51(3).

[7] S. Laws, E. Eberhardt, S. Loew, F. Descoeudres. Geomechanical properties of shear zones in the Eastern Aar Massif, Switzerland and their implication on tunnelling. Rock Mech Rock Eng. 2003;36(4):271-303.

[8] D. Wise, D. Dunn, J. Engelder, P. Geiser, R. Hatcher, S. Kish. *Fault-related rocks: suggestions for terminology. Geology*. 1984;12(7):391-4.

[9] S. Vearncombe, J. R. Vearncombe. *Tectonic controls on kimberlite location, southern Africa. J Struct Geol*. 2002;24(10):1619-25.

[10] S.D. Priest. *Discontinuity analysis for rock engineering*. Springer Science & Business Media; 2012.

[11] D. Laubscher, J. Jakubec. *The MRMR rock mass classification for jointed rock masses.* Underground Mining Methods: Engineering Fundamentals and International Case Studies, WA Hustrulid and RL Bullock (eds) Society of Mining Metallurgy and Exploration, SMME. 2001:475-81.

[12] Z. T. Bieniawski, 1973. *Engineering classification of jointed rock masses*. Trans S. Afr. Inst. Civ. Engrs 15, 335-344.

[13] J. A. Hudson, S. D. *Priest, Discontinuities and Rock Mass Geometry,* International Journal of Rock Mechanics and Mining Sciences, 1979: Vol: 16, Pages: 339-362, ISSN: 0148-9062.

[14] D. U. Deere, R. Miller. *Engineering classification and index properties for intact rock*. 1966.

[15] E. Hoek, P. Marinos. *Predicting tunnel squeezing problems in weak heterogeneous rock masses*. Tunnels and tunnelling international. 2000;32(11):45-51.

[16] E. Hoek, T. Carter, M. Diederichs. *Quantification of the geological strength index chart*. 47th US Rock Mechanics/Geomechanics Symposium; American Rock Mechanics Association; 2013.

[17] E. Hoek, E.T. Brown. *Practical estimates of rock mass strength*. Int J Rock Mech Min Sci. 1997;34(8):1165-86.

[18] E. Hoek, C. Carranza-Torres, B. Corkum. *Hoek-Brown failure criterion-2002 edition*. Proceedings of NARMS-Tac. 2002;1:267-73.

[19] D. Laubscher D. *A geomechanics classification system for the rating of rock mass in mine design*. JS Afr.Inst.Metall. 1990;90(10):267-73.

[20] P. Wriggers. *Finite element algorithms for contact problems.* Archives of Computational Methods in Engineering. 1995;2(4):1-49.

[21] S. Bandis, A. Lumsden, N. Barton. *Fundamentals of rock joint deformation*. International Journal of Rock Mechanics and Mining Sciences & Geomechanics Abstracts; Elsevier; 1983.

[22] https://www.rocscience.com/ Accessed on 27/11/2016

[23] Y. Zheng, X. Tang, S. Zhao, C. Deng, W. Lei. *Strength reduction and step-loading finite element approaches in geotechnical engineering*. Journal of Rock Mechanics and Geotechnical Engineering. 2009 10/26;1(1):21-30.